THE JOURNAL OF BIOLOGICAL CHEMISTRY VOL. 283, NO. 14, pp. 8919–8929, April 4, 2008

Tor Pathway Control of the Nitrogen-responsive *DAL5* Gene Bifurcates at the Level of Gln3 and Gat1 Regulation in *Saccharomyces cerevisiae*[*] [S]

Received for publication, October 25, 2007, and in revised form, January 15, 2008 Published, JBC Papers in Press, February 1, 2008, DOI 10.1074/jbc.M708811200

Isabelle Georis[‡1], Jennifer J. Tate[§2], Terrance G. Cooper[§2,3], and Evelyne Dubois[‡1]

From the [‡]Institut de Recherches Microbiologiques J.-M. Wiame, Laboratoire de Microbiologie Université Libre de Bruxelles, B1070 Brussels, Belgium and the [§]Department of Molecular Sciences, University of Tennessee, Memphis, Tennessee 38163

The Tor1,2 protein kinases globally influence many cellular processes including nitrogen-responsive gene expression that correlates with intracellular localization of GATA transcription activators Gln3 and Gat1/Nil1. Gln3-Myc^{13} and Gat1-Myc^{13} are restricted to the cytoplasm of cells provided with good nitrogen sources, *e.g.* glutamine. Following the addition of the Tor1,2 inhibitor, rapamycin, both transcription factors relocate to the nucleus. Gln3-Myc^{13} localization is highly dependent upon Ure2 and type 2A-related phosphatase, Sit4. Ure2 is required for Gln3 to be restricted to the cytoplasm of cells provided with good nitrogen sources, and Sit4 is required for its location to the nucleus following rapamycin treatment. The paucity of analogous information concerning Gat1 regulation prompted us to investigate the effects of deleting *SIT4* and *URE2* on Gat1-Myc^{13} localization, DNA binding, and NCR-sensitive transcription. Our data demonstrate that Tor pathway control of NCR-responsive transcription bifurcates at the regulation of Gln3 and Gat1. Gat1-Myc^{13} localization is not strongly influenced by deleting *URE2*, nor is its nuclear targeting following rapamycin treatment strongly dependent on Sit4. ChIP experiments demonstrated that Gat1-Myc^{13} can bind to the *DAL5* promoter in the absence of Gln3. Gln3-Myc^{13}, on the other hand, cannot bind to *DAL5* in the absence of Gat1. We conclude that: (i) Tor pathway regulation of Gat1 differs markedly from that of Gln3, (ii) nuclear targeting of Gln3-Myc^{13} is alone insufficient for its recruitment to the *DAL5* promoter, and (iii) the Tor pathway continues to play an important regulatory role in NCR-sensitive transcription even after Gln3-Myc^{13} is localized to the nucleus.

Increasing use of rapamycin analogues clinically and in Phase II and III clinical trials has greatly stimulated investigation of its cellular target mTor (1–4). This global regulator influences many cellular processes, and the model organism, *Saccharomyces cerevisiae* has been particularly useful in elucidating the biochemical mechanisms through which such regulation is achieved. In contrast with higher eukaryotes, *S. cerevisiae* contains two Tor serine/threonine protein kinases, Tor1 and Tor2 (5–7). Activities of the nitrogen catabolite repression (NCR)-sensitive[4] GATA family transcription activators, Gln3 and Gat1, have been used as downstream reporters of Tor1,2-mediated gene regulation, and this has increased interest in their regulation as well (8–16). The utility of GATA factor localization as a Tor reporter derives from the correlation that Gln3 and Gat1 respond similarly to rapamycin inhibition of Tor1,2, to nitrogen starvation, or when cells are provided with a poor nitrogen source (proline); they localize to the nucleus, and NCR-sensitive transcription increases. On the other hand, with good nitrogen sources (*e.g.* glutamine and in some strains ammonia), transcription of NCR-sensitive genes encoding proteins required for the transport and utilization of poor nitrogen sources is minimal, which correlates with Gln3-Myc^{13} and Gat1-Myc^{13} being sequestered in the cytoplasm, a response that, in the case of Gln3, requires Ure2 (8–18). The findings that Gln3 interacts with Ure2 *in vivo* and can be isolated as a Gln3-Ure2 complex *in vitro* extended the above correlations and offered a possible mechanism of how cytoplasmic sequestration of the GATA factors might be achieved (8, 11, 19, 20).

These and other correlations led to the proposal that excess nitrogen activates Tor1,2 (8–14, 21–24), although the precise mechanism remains unknown. They in turn phosphorylate Tap42, which inhibits the protein phosphatase Sit4. Upon rapamycin treatment, Tor is inactivated, and Tap42 dissociates from Sit4, which dephosphorylates Gln3 and thereby dissociates the Gln3-Ure2 complex. Dephosphorylated Gln3 can then enter the nucleus and mediate NCR-sensitive transcription. Gat1 was reported to be similarly regulated (8). Subsequently, protein kinase Npr1 was posited to be a negative regulator of nuclear Gln3 localization (25).

This model has stimulated detailed studies of the steps outlined above. Although intracellular Gln3 phosphorylation and localization sometimes positively correlated, as predicted by the model of Tor pathway structure and operation, in other cases experimental observations were inconsistent with the

[*] The costs of publication of this article were defrayed in part by the payment of page charges. This article must therefore be hereby marked "*advertisement*" in accordance with 18 U.S.C. Section 1734 solely to indicate this fact.

This article is dedicated to Prof. Ronald Butow of the University of Texas Southwestern Medical Center (1936–2007), who contributed so much to the field of mitochondrial retrograde regulation and its interface with nitrogen and GATA factor regulation in *S. cerevisiae*.

[S] The on-line version of this article (available at http://www.jbc.org) contains supplemental Figs. S1 and S2.

[1] Supported by the Commission Communautaire Française.

[2] Supported by National Institutes of Health Grant GM-35642 and National Institutes of Health/National Science Foundation Grant DMS-0443901.

[3] To whom correspondence should be addressed. Fax: 901-448-8462; E-mail: tcooper@utmem.edu.

[4] The abbreviations used are: NCR, nitrogen catabolite repression; IN, input; IP, immunoprecipitated; RT, reverse transcription; DAPI, 4′,6′-diamino-2-phenylindole; ChIP, chromatin immunoprecipitation.

predictions. Detailed investigations of expected correlations that failed to occur repeatedly led to alternative explanations of existing data and concomitantly revised and increased our understanding of Tor1,2 and GATA factor regulation. Among the most important findings have been the observations that: (i) in its active form, Sit4 is in a complex with Tap42 (21, 22, 27); (ii) although methionine sulfoximine, an inhibitor of glutamine biosynthesis, and rapamycin treatment both cause nuclear Gln3-Myc^{13} localization (28, 29), they produce opposite effects on Gln3-Myc^{13} phosphorylation, *i.e.* the former increases phosphorylation, whereas the latter decreases it (29); (iii) Sit4 remains active with respect to Gln3 dephosphorylation in the presence of both good and poor nitrogen sources, *i.e.* its activity is not demonstrably nitrogen source-responsive (30); (iv) nitrogen source-dependent changes in Gln3-Myc^{13} phosphorylation become demonstrable when *SIT4* is deleted, suggesting that nitrogen-responsive protein kinase activity rather than Sit4 phosphatase activity is the primary determining link between nitrogen availability and Gln3-Myc^{13} phosphorylation (30); and (v) Npr1 protein kinase participates in Gln3 regulation indirectly by influencing the uptake of ammonia (31, 32).

The studies described above evaluated the influence of nutrients, Tor1,2 inhibitors, and type 2A-related phosphatase activities (Sit4, Pph3) on Gln3-Myc^{13} phosphorylation and localization. Missing from these analyses, however, are data that analyze and correlate the requirements of GATA factor localization with *in vivo* DNA binding and NCR-sensitive transcription. Also missing are data that address the regulation of Gat1. Although Gat1 was concluded to be regulated analogously to Gln3 (8), several predicted responses have eluded demonstration (8). Gat1-mediated transcription is NCR-sensitive, but it has not yet been possible to demonstrate a Gat1-Ure2 complex *in vitro* (7, 8, 33). Further, nitrogen source or rapamycin-dependent changes in Gat1-Myc^{13} phosphorylation have not been demonstrated, even though changes in Gat1-Myc^{13} phosphorylation in response to carbon starvation can be readily observed (33).

To provide the missing information cited above, we investigated the requirements of type 2A-related phosphatases (Sit4 and Pph3) for NCR-sensitive gene expression and compared them with those expected from previous studies of Gln3-Myc^{13} localization (30). This led us to investigate rapamycin-induced Gat1-Myc^{13} localization, DNA binding, and NCR-sensitive transcription in wild type and type 2A-related phosphatase mutant strains. These investigations demonstrate that Tor1,2 pathway regulation of NCR-sensitive gene transcription bifurcates at the level of the GATA factors Gln3 and Gat1.

MATERIALS AND METHODS

Strains and Culture Conditions: S. cerevisiae—Strains used in this work are listed in Table 1. Growth conditions were identical to those described in Tate *et al.* (30) and Scherens *et al.* (34). Rapamycin (Sigma and LC Laboratories) and methionine sulfoximine (Sigma) were prepared as described earlier (30) and used as indicated in the figure legends.

Strain Construction—Deletion strains involving insertion of kanMX or natMX cassettes were constructed using the long flanking homology strategy of Wach (35), as described in Tate *et al.* (30). Chromosomal *GLN3* or *GAT1* were tagged at their C termini with 13 copies of the Myc epitope (Myc^{13}) as described by Longtine *et al.* (36), using primers 5′-agcaattgctgacgaattggattggttaaaatttggtataCGGATCCCCGGGTTAATTAA-3′ (GLN3-F2) and 5′-TTATTAACATAATAAGAATAATGATAATGATAATACGCGGgaattcgagctcgtttaaac-3′ (GLN3-R1) for *GLN3* and 5′-AAATGGCAATCTGAGCCTGGATTGGTTGAATCTGAATTTACGGATCCCCGGGTTAATTAA-3′ (GAT1-F2) and 5′-CATGGAAAGAAGCGAGTACTTTTTTTTTTTTGGGGGATCTAGAATTCGAGCTCGTTTAAAC-3′ (GAT1-R1) for *GAT1*.

Northern Blot Analysis—Total RNA was extracted as described earlier (37). Northern blot analysis was performed as described by Foury and Talibi (38). Digoxigenin DNA probes (about 500 bp) were synthesized by PCR, using primers 5′-AGTGTTGTCACACCTTGC-3′ and 5′-ACCCATTAATAGGGTTTC-3′ for *DAL5* and 5′-AAACAGCAAGAAAGTCCACTGG-3′ and 5′-ACCTCTTAATCTTCTAGCCAAC-3′ for *HHT1* and labeled using a PCR digoxigenin probe synthesis kit (Roche Applied Science). Treatment of the Hybond-N+ nylon membranes was as described earlier (31).

Chromatin Immunoprecipitation—The cells (100-ml cultures grown to an absorbance ($A_{660\,nm} = 0.6$) corresponding to 6×10^6 cells/ml) were treated with 1% formaldehyde for 30 min at 25 °C and mixed by orbital shaking. Glycine was then added to a final concentration of 500 mM and incubation continued for 5 min. The cells were collected, washed once with cold 10 mM Tris-HCl, pH 8, washed once with cold FA-SDS buffer (50 mM HEPES-KOH, pH 7.5, 150 mM NaCl, 1 mM EDTA, 1% Triton X-100, 0.1% sodium deoxycholate, 0.1% SDS, 1 mM phenylmethylsulfonyl fluoride), and resuspended in 1 ml of cold FA-SDS buffer. An equal volume of glass beads (0.5 mm in diameter) was added, and the cells were disrupted by vortexing for 30 min in a cold room. The lysate was diluted into 4 ml of FA-SDS buffer, and the glass beads were discarded. The cross-linked chromatin was then pelleted by centrifugation (17,000 × *g* for 35 min), washed for 60 min with FA-SDS buffer, resuspended in 1.6 ml of FA-SDS buffer for 15 min at 4 °C, and sonicated three times for 30 s. each (Branson Sonifier 250, Pulse 60%, Power 2) to yield an average DNA fragment size of 700 base pairs. Finally, the sample was clarified by centrifugation at 14,000 × *g* for 30 min and diluted 4-fold in FA-SDS buffer, and aliquots of the resultant chromatin containing solution were stored at −80 °C.

Myc^{13}-tagged proteins were immunoprecipitated by incubating 100 μl of the chromatin containing solution for 180 min at 4 °C with 2 μl of mouse anti-Myc antibodies (Santa Cruz) prebound to 10 μl of Dynabeads Pan Mouse IgG (Dynal) according to the manufacturer's instructions. Immune complexes were washed six times in FA-SDS buffer and recovered by treating with 50 μl of Pronase Buffer (25 mM Tris, pH 7.5, 5 mM EDTA, 0.5% SDS) at 65 °C with agitation. Input (IN) and immunoprecipitated (IP) fractions were then subjected to Pronase treatment (0.5 mg/ml; Roche Applied Science) for 60 min at 37 °C, and formaldehyde cross-links were reversed by incubating the eluates overnight at 65 °C. Finally, the samples were treated with RNase (50 μg/ml) for 60 min at 37 °C. DNA from the IP fractions was purified using the High Pure PCR Product

TABLE 1
Strains used in the work

Strain	Background	Parent	Genotype	Primer
TB50	TB	(12)	*MATa, leu2-3,112, ura3-52, trp1, his3, rme1, HMLa*	None
TB123	TB	(12)	*MATa, leu2-3, 112, ura3-52, rme1, trp1, his4, GAL$^+$, HMLa, GLN3-MYC^{13}[KanMX]*	None
TB136-2a	TB	(12)	*MATa, leu2-3,112, ura3-52, rme1, trp1, his4, GAL$^+$, HMLa, GLN3-MYC^{13}[KanMX], sit4::kanMX*	None
TB138-1a	TB	(12)	*MATa, leu2-3,112, ura3-52, rme1, trp1, his4, GAL$^+$, HMLa, ure2::URA3, GLN3-MYC^{13}[KanMX]*	None
FV003	TB	TB123	*MATa, leu2-3, 112, ura3-52, rme1, trp1, his4, GAL$^+$, HMLa, GLN3-MYC^{13}[KanMX], pph3::natMX*	*pph3*: 5′, −400 to −379 and −22 to −1 3′ 927 to 950 and 1206 to 1228
FV004	TB	TB136-2a	*MATa, leu2-3,112, ura3-52, rme1, trp1, his4, GAL$^+$, HMLa, GLN3-MYC^{13}[KanMX], sit4::kanMX, pph3::natMX*	*pph3*: 5′, −400 to −379 and −22 to −1 3′ 927 to 950 and 1206 to 1228
FV005	TB	TB50	*MATa, leu2-3,112, ura3-52, trp1, his3, rme1, HMLa, gln3::kanMX*	*gln3*: 5′, −438 to −421 and −15 to −1 3′ 2194 to 2211 and 2597 to 2614
FV006	TB	TB50	*MATa, leu2-3,112, ura3-52, trp1, his3, rme1, HMLa, gat1::natMX*	*gat1*: 5′, −422 to −405 and −15 to −1 3′ 1534 to 1555 and 1879 to 1896
FV008	TB	TB136-2a	*MATa, leu2-3,112, ura3-52, rme1, trp1, his4, GAL$^+$, HMLa, GLN3-MYC^{13}[KanMX], sit4::kanMX, gat1::natMX*	*gat1*: 5′, −422 to −405 and −15 to −1 3′ 1534 to 1555 and 1879 to 1896
FV018	TB	TB123	*MATa, leu2-3, 112, ura3-52, rme1, trp1, his4, GAL$^+$, HMLa, GLN3-MYC^{13}[KanMX], gat1::natMX*	*gat1*: 5′, −422 to −405 and −15 to −1 3′ 1534 to 1555 and 1879 to 1896
FV029	TB	TB50	*MATa, leu2-3,112, ura3-52, trp1, his3, rme1, HMLa, sit4::natMX*	*sit4*: 5′, −450 to −429 and −23 to −1 3′ 937 to 955 and 1380 to 1400
FV030	TB	TB50	*MATa, leu2-3,112, ura3-52, trp1, his3, rme1, HMLa, sit4::natMX, gln3::kanMX*	*sit4*: 5′, −450 to −429 and −23 to −1 3′ 937 to 955 and 1380 to 1400 *gln3*: 5′, −438 to −421 and −15 to −1 3′ 2194 to 2211 and 2597 to 2614
FV063	TB	TB50	*MATa, leu2-3,112, ura3-52, trp1, his3, rme1, HMLa, GAT1-MYC^{13}[HIS3]*	5′ GAT1-F2, 3′ GAT1-R1
FV064	TB	FV005	*MATa, leu2-3,112, ura3-52, trp1, his3, rme1, HMLa, gln3::kanMX, GAT1-MYC^{13}[HIS3]*	5′ GAT1-F2, 3′ GAT1-R1
FV065	TB	FV063	*MATa, leu2-3,112, ura3-52, trp1, his3, rme1, HMLa, GAT1-MYC^{13}[HIS3], pph3::natMX*	*pph3*: 5′, −400 to −379 and −22 to −1 3′ 927 to 950 and 1206 to 1228
FV066	TB	FV063	*MATa, leu2-3,112, ura3-52, trp1, his3, rme1, HMLa, GAT1-MYC^{13}[HIS3], sit4::kanMX*	*sit4*: 5′, −450 to −429 and −23 to −1 3′ 937 to 955 and 1380 to 1400
FV067	TB	FV063	*MATa, leu2-3,112, ura3-52, trp1, his3, rme1, HMLa, GAT1-MYC^{13}[HIS3], pph3::natMX, sit4::kanMX*	*pph3*: 5′, −400 to −379 and −22 to −1 3′ 927 to 950 and 1206 to 1228 *sit4*: 5′, −450 to −429 and −23 to −1 3′ 937 to 955 and 1380 to 1400
FV071	TB	TB136-2a	*MATa, leu2-3,112, ura3-52, rme1, trp1, his4, GAL$^+$, HMLa, ure2::natMX, GLN3-MYC^{13}[KanMX], sit4::kanMX*	*ure2*: 5′, −300 to −279 and −21 to −1 3′ 1066 to 1084 and 1325 to 1345
FV072	TB	TB138-1a	*MATa, leu2-3,112, ura3-52, rme1, trp1, his4, GAL$^+$, HMLa, ure2::URA3, GLN3-MYC^{13}[KanMX], sit4::natMX*	*sit4*: 5′, −450 to −429 and −23 to −1 3′ 937 to 955 and 1380 to 1400
FV088	TB	FV063	*MATa, leu2-3,112, ura3-52, trp1, his3, rme1, HMLa, GAT1-MYC^{13}[HIS3], ure2::natMX*	*ure2*: 5′, −300 to −279 and −21 to −1 3′ 1066 to 1084 and 1325 to 1345
FV089	TB	FV066	*MATa, leu2-3,112, ura3-52, trp1, his3, rme1, HMLa, GAT1-MYC^{13}[HIS3], sit4::kanMX, ure2::natMX*	*ure2*: 5′, −300 to −279 and −21 to −1 3′ 1066 to 1084 and 1325 to 1345

Purification Kit (Roche Applied Science) and eluted in 50 μl of 20 mM Tris buffer, pH 8. IN fractions were boiled 10 min and diluted 500-fold with no further purification prior to quantitative PCR analysis.

Concentrations of specific DNA targets in IN and IP samples were measured by real time PCR using a LightCycler 1.5 instrument and the FastStart DNA Master Plus SYBR Green I kit according to the manufacturer's (Roche Applied Science) protocol. Primers amplified a 161-bp region in the promoter of *DAL5* (DAL5P1, 5′-CGAGGAGCTATCATTTGCTG-3′; DAL5P2, 5′-ATCTTTTGCCCCGATAATCC-3′) or a 150-bp region 2.5 kb upstream of the *DAL5* AUG as the unbound control (DAL5U1, 5′-GTTCATTAGTCGCCTACAGC-3′; DAL5U2, 5′-CAGAGCCCCGCATATTTTGA-3′). A standard curve was generated for each primer pair with five successive 10-fold dilutions of an IN sample. This standard curve was used to assess PCR efficiency and determine the relative concentration of target DNA in all other samples. Specificity of the PCR products was assessed by melting curve analysis. Primer pairs generating different products, identified by more than one melting temperature peak, were discarded.

The data were analyzed with LightCycler software, version 5.32. The IP/IN ratio corresponds to the concentration of target DNA in the IP sample relative to that in the corresponding IN sample, multiplied by 10. IP/IN values obtained for the unbound control (DAL5U) were substracted from IP/IN values obtained for the *DAL5* promoter (DAL5P). To counterbalance variation generated by the immunoprecipitation step, we treated all of our data as follows. The wild type-induced value was set as 1, and the IP/IN value of every simultaneously immunoprecipitated sample was normalized accordingly. For every independent culture, the mean of the IP/IN ratios for two to four replicate immunoprecipitations was calculated. The values in Figs. 4 and 7 correspond to the mean IP/IN value of at least two independent cultures. The mean normalized IP/IN values of both DAL5U and DAL5P are displayed in the supplemental material.

Quantitative RT-PCR—cDNA was generated from 100–500 ng of total RNA using a Transcriptor First Strand cDNA synthesis kit (Roche Applied Science) with oligo(dT) as primer following the manufacturer's recommended protocol. cDNAs were quantified by real time PCR as described above. Primers amplified a 154-bp region of *DAL5* (DAL5O1, 5′-TTCGAATGCTTCCCTAGACG-3′; DAL5O2, 5′-CTTCATGGCCTCATCAACCT-3′) or a 125-bp region of *TBP1* (TBP1O1, 5′-TATAACCCCAAGCGTTTTGC-3′; TBP1O2, 5′-GCCAGCTTT-

GAGTCATCCTC-3′). Expression values correspond to the ratio of *DAL5*- over *TBP1*-specific mRNAs determined in each sample.

Indirect Immunofluorescence Microscopy—Cell collection and fixation for indirect immunofluorescence was performed using the method of Cox *et al.* (39) as modified by Tate *et al.* (30, 32). Gln3-Myc^{13} localization was visualized using primary monoclonal antibody 9E10 (c-Myc; Covance MMS-150P) at a dilution of 1:1000 and 1:5000 for Gat1-Myc^{13} visualization. Alexa Fluor 594 goat anti-mouse IgG antibody (Molecular Probes, at a dilution of 1:200) was used as secondary antibody in both cases. DNA was visualized using 4′,6′-diamino-2-phenylindole (DAPI) contained in the mounting medium (Sigma) (39). Some strains, those containing the *sit4*Δ and especially mutant strains containing *GAT1-MYC*^{13}, required greater amounts of zymolyase and/or times of digestion to achieve high quality results.

The cells were imaged using a Zeiss Axioplan 2 imaging microscope with a 100× Plan-Apochromat 1.40 oil objective at room temperature. The images were acquired using a Zeiss Axio camera and AxioVision 3.0 and 4.6.3 (Zeiss; 4, 2007) software, processed with Adobe Photoshop and Illustrator programs. Gamma settings were altered where necessary to decrease background fluorescence in areas that did not contain cells and to avoid any change or loss in cellular detail. Changes were applied uniformly to the image presented.

Determination of Intracellular Gln3-Myc^{13} and Gat1-Myc^{13} Distribution—To provide more representative and complete descriptions of Gln3-Myc^{13} and Gat1-Myc^{13} behavior than obtainable from an isolated image, we manually scored Gln3-Myc^{13} or Gat1-Myc^{13} localization in 200 or more cells in multiple, randomly chosen microscopic fields from which each image presented was taken. Scoring was performed exclusively using unaltered primary image files viewed with Zeiss AxioVision 3.0 and 4.6.3 software. The cells were classified into one of three categories: cytoplasmic (cytoplasmic fluorescence only), nuclear-cytoplasmic (fluorescence appeared in the cytoplasm as well as co-localizing with DAPI-positive material), and nuclear (co-localizing only with DAPI-positive material). Although scoring limitations and reproducibility were described in Tate *et al.* (30, 32), we emphasize again, as we did earlier (40), that the nuclear-cytoplasmic category is, of necessity, arbitrary. Placing cells in that category is based on subjective visual evaluation by the individual scoring the cells; it is not an objective instrument-based measurement. When the fluorescent signal is not restricted to a single cellular compartment, scoring depends upon repeated decisions of whether it is nuclear-cytoplasmic or a category flanking it. They will undoubtedly differ in detail from those of another observer, who sets their category dividing lines differently. Although our intracellular distributions were scored as consistently as possible, conclusions are most prudently made when primarily based on straightforwardly detected changes in overall distribution patterns that are apparent in the microscopic images. Similar experiments were generally repeated two or more times with similar results. Experiment to experiment variation can be ascertained by comparing similar experimental conditions in this work and previous work (30, 32, 40). During this work, we noticed that unless the fluorescent signal was exclusively localized to a single cellular compartment, there was greater variability in scoring Gat1-Myc^{13} than Gln3-Myc^{13}.

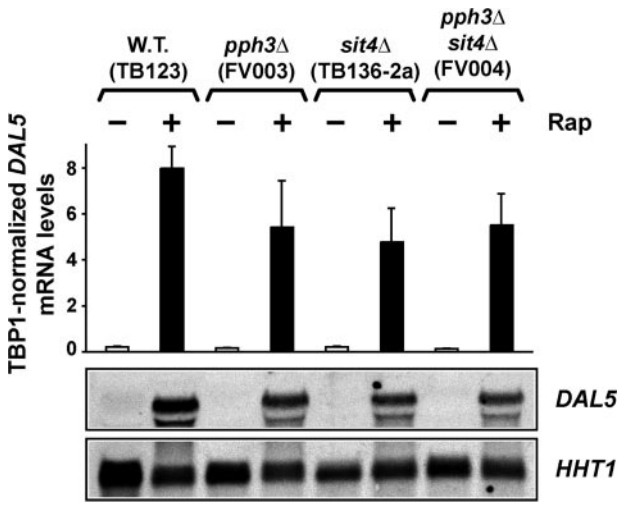

FIGURE 1. **Effect of deleting type 2A-related phosphatase genes *SIT4* and *PPH3* on rapamycin-induced *DAL5* expression.** Total RNA was isolated from wild type (TB123), *pph3*Δ (FV003), *sit4*Δ (TB136-2a), and *pph3*Δ *sit4*Δ (FV004) cells expressing *GLN3-MYC*^{13} that replaced the native *GLN3* gene. Cells were grown in YNB-glutamine medium and treated with rapamycin (*Rap*) (0.2 μg/ml) for 30 min. Control cells were similarly grown but untreated. *DAL5* mRNA levels were quantified by quantitative RT-PCR, as described under "Materials and Methods." *DAL5* values were normalized with *TBP1*. The values represent the averages of at least three experiments from independent cultures, and the *error bars* indicate standard errors. 30 μg of total RNA from each sample were subjected to Northern blot analysis. *HHT1* was used as the loading and transfer efficiency control.

RESULTS

Type 2A-related Phosphatase (Sit4 and Pph3) Requirements for Rapamycin-induced DAL5 Transcription—Our studies began by evaluating the type 2A-related Sit4 and Pph3 protein phosphatase requirements of *DAL5* gene expression. This permitted comparisons with previously obtained information about Gln3-Myc^{13} localization and the ability to test predictions generated by it. Wild type (TB123) and isogenic *pph3*Δ (FV003), *sit4*Δ (TB136-2a), and *pph3*Δ *sit4*Δ (FV004) strains were grown in YNB-glutamine medium to mid-log phase ($A_{660\,nm}$ = 0.6). Following a 30-min treatment with 0.2 μg/ml rapamycin, expression of *DAL5*, a representative NCR-sensitive gene, was analyzed by quantitative RT-PCR and Northern blot assays (Fig. 1). As expected, *DAL5* expression in untreated cells was minimal in all four strains, *i.e.* NCR-sensitive transcription was repressed because of growth with a good nitrogen source (Fig. 1). Quite surprisingly, however, rapamycin-induced *DAL5* expression was only slightly reduced in all three mutants, demonstrating that Sit4 and Pph3 were dispensable (Fig. 1). This lack of a Sit4 requirement differed sharply from the absolute Sit4 requirement previously shown for rapamycin-induced nuclear Gln3-Myc^{13} localization under identical conditions (see Figs. 4 and 5 of Ref. 30). The presence of rapamycin-induced *DAL5* transcription in *sit4*Δ cells, where Gln3-Myc^{13} was excluded from the nucleus, suggested that our current view of Tor1,2 regulation of NCR-sensitive (*DAL5*) transcription required revision.

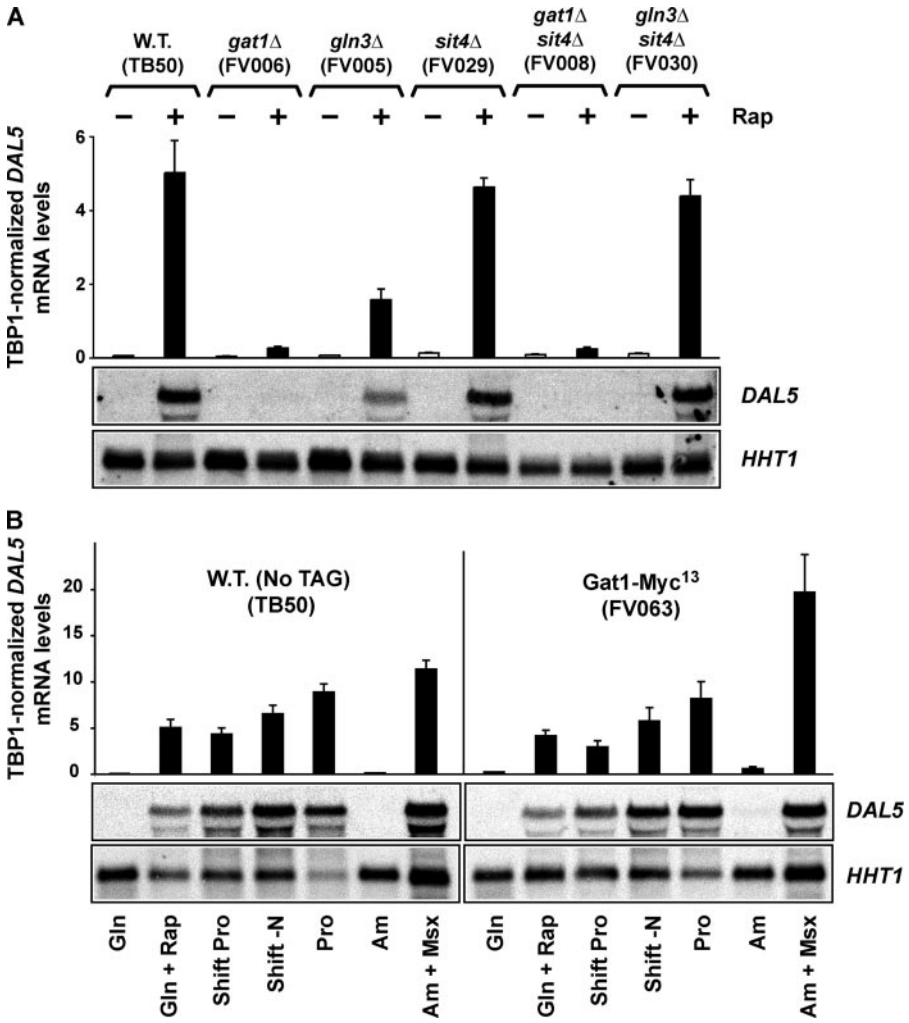

FIGURE 2. *A*, relative contributions of Gat1 and Gln3 to rapamycin-induced *DAL5* expression. Total RNA was isolated from wild type (TB50), *gat1*Δ (FV006), *gln3*Δ (FV005), *sit4*Δ (FV029), *gat1*Δ*sit4*Δ (FV008), and *gln3*Δ*sit4*Δ (FV030) cultures grown in YNB-glutamine medium. The cells were treated and analyses performed as in Fig. 1. *B*, functionality and normal regulation of the integrated GAT1-MYC^{13} construct. Total RNA was isolated from wild type (TB50) and wild type *GAT1-MYC*^{13} (FV063) cells grown in glutamine (*Gln*) medium in the presence or absence of 0.2 μg/ml rapamycin (*Rap*) for 30 min, 60 min after transfer from glutamine to proline (*shift Pro*), or nitrogen-free medium (*shift -N*), proline (*Pro*), or ammonium (*Am*) medium in the presence or absence of 2 mM methionine sulfoximine (*Msx*) for 20 min. The cells were treated and analyses performed as in Fig. 1. *W.T.*, wild type.

The most plausible explanation of rapamycin-responsive *DAL5* transcription in the *sit4*Δ was that it derived from a transcription factor other than Gln3. Gat1 was the most likely candidate to support this transcription because it had been previously shown to mediate NCR-sensitive gene expression, to be regulated by Tor1,2, and hence to be responsive to rapamycin treatment (5, 7, 17, 18, 41–44). To test this hypothesis, we measured the individual contributions of Gln3 and Gat1 to *DAL5* transcription. Deleting *GLN3* (*gln3*Δ, FV005) reduced rapamycin-induced *DAL5* expression to about a third of the wild type (TB50) level (Fig. 2*A*). This, however, was a much weaker effect than the essentially background levels observed when *GAT1* was deleted (Fig. 2*A*, *gat1*Δ, FV006). Positively correlating with these observations, rapamycin-induced *DAL5* transcription was also absent in a *sit4*Δ*gat1*Δ (FV008), but unaffected in a *sit4*Δ*gln3*Δ (FV030). In fact, additionally deleting *SIT4* in a *gln3*Δ inexplicably suppressed the effect of the *gln3*Δ. Thus, Gat1 activated *DAL5* expression following rapamycin treatment and did not require Sit4 activity to do so.

Rapamycin-induced Nuclear Gat1-Myc^{13} *Localization Is Largely Sit4-independent*—The above observations suggested that rapamycin-induced nuclear Gat1-Myc^{13} localization might possess different protein phosphatase (Sit4, Pph3) requirements than Gln3-Myc^{13} and that the Tor signal transduction pathway bifurcated at the control of GATA factor localization. To test these suggestions directly, we replaced chromosomal *GAT1* with *GAT1-MYC*^{13}. Before further analyses, however, we used quantitative RT-PCR and Northern blot assays to validate the functionality and native regulation of the construct (Fig. 2*B*). Steady state *DAL5* mRNA levels were comparable in wild type untagged (TB50) and Gat1-Myc^{13}-tagged (FV063) cells cultured under conditions previously used to analyze Gln3-Myc^{13} localization (30). Thus, by these criteria, our Myc^{13}-tagged Gat1 protein was normally regulated.

We then used the *GAT1-MYC*^{13} constructs to evaluate intracellular Gat1-Myc^{13} localization in glutamine-grown, rapamycin-treated wild type (FV063), *sit4*Δ (FV066), *pph3*Δ (FV065), and *sit4*Δ*pph3*Δ (FV067) cells. Rapamycin induced nuclear localization of Gat1-Myc^{13} in glutamine-grown wild type cells (Fig. 3, *A* and *B*, *W.T.*). However, unlike the situation with Gln3-Myc^{13} (Figs. 4 and 5 of Ref. 30), deleting *SIT4* only modestly reduced nuclear Gat1-Myc^{13} localization following rapamycin treatment. This concomitantly increased the number of cells in which Gat1-Myc^{13} was nuclear-cytoplasmic (Fig. 3, *A* and *B*, *sit4*Δ) but not those in which Gat1-Myc^{13} was exclusively localized to the cytoplasm. This localization profile closely paralleled the limited decrease in *DAL5* expression observed in the *sit4*Δ (Fig. 1) and led us to conclude that nuclear Gat1-Myc^{13} localization possessed at most only a limited Sit4 requirement rather than the absolute requirement observed for Gln3-Myc^{13}. Deletion of *PPH3*, either alone or in conjunction with *SIT4*, did not yield a phenotype that significantly differed from a wild type in the former case or a *sit4*Δ in the latter (Fig. 3, *A* and *B*, *pph3*Δ and *pph3*Δ*sit4*Δ). This argued that, as occurred with Gln3-Myc^{13}, Pph3 did not play a demonstrable role in nuclear Gat1-Myc^{13} localization under these conditions.

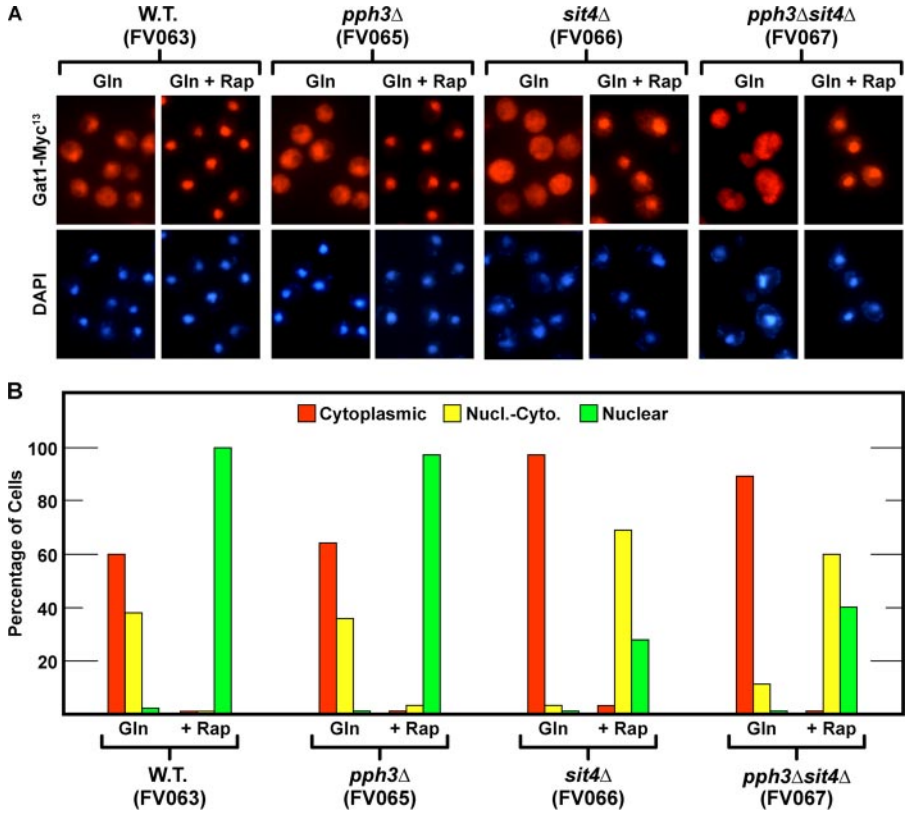

FIGURE 3. **Effects of rapamycin on the intracellular localization of Gat1-Myc^{13} in wild type, *sit4*Δ, and *pph3*Δ strains.** Wild type (*W.T.*) and mutant strains were grown in YNB-glutamine medium. Split cultures were left untreated (*Gln*) or treated with rapamycin (0.2 μg/ml) for 20 min (+*Rap*), sampled, and processed for immunofluorescence microscopy as described under "Materials and Methods." Strain numbers appear below the pertinent genotype. The images are presented in pairs with Gat1-Myc^{13}-dependent fluorescence above and DAPI-stained cells below. The images and corresponding histograms below them were taken from the same slides. Intracellular distributions of Gat1-Myc^{13} (using criteria described under "Materials and Methods") are indicated by the bar color in the histograms: *red*, cytoplasmic; *yellow*, nuclear-cytoplasmic; *green*, nuclear.

Additional smaller differences appeared when Gln3-Myc^{13} and Gat1-Myc^{13} localization data were compared (compare Figs. 4 and 5 in Ref. 30 with Fig. 3 of this work). Fluorescence signals emanating from Gat1-Myc^{13} were stronger than those from Gln3-Myc^{13}, and Gat1-Myc^{13} was somewhat more nuclear under most conditions. For example, Gln3-Myc^{13} could not be detected in the nuclei of glutamine-grown wild type cells (Figs. 4 and 5 of Ref. 30), whereas Gat1-Myc^{13} was frequently observed to be nuclear-cytoplasmic (Fig. 3, *A* and *B*, *W.T. Gln*). This correlated with earlier observations that Gat1-dependent transcription was less NCR-sensitive than that mediated by Gln3 (41–44). Additionally, Gat1-Myc^{13} was nuclear in nearly all rapamycin-treated, glutamine-grown wild type cells, whereas Gln3-Myc^{13} was more nuclear-cytoplasmic (Figs. 4 and 5 of Ref. 30). Overall, rapamycin generated a stronger response with Gat1-Myc^{13} than Gln3-Myc^{13}. We also observed greater variability in data scoring Gat1-Myc^{13} localization in glutamine-grown but not rapamycin-treated wild type cells than we had previously encountered with Gln3-Myc^{13}.

Gat1-Myc^{13} and Gln3-Myc^{13} Possess Different Requirements for Rapamycin-induced Binding to the DAL5 Promoter—The previous view that Gln3 and Gat1 were similarly regulated was challenged by the strikingly different Sit4 requirements they possessed for rapamycin-induced nuclear localization. Therefore, we used chromatin immunoprecipitation (ChIP) assays to determine whether these differences extended to GATA factor binding to the NCR-sensitive *DAL5* promoter. Gat1-Myc^{13} was effectively recruited to the promoter of rapamycin-treated, glutamine-grown wild type (FV063), *gln3*Δ (FV064), and *sit4*Δ (FV066) cells (Fig. 4*A* and supplemental Fig. S1). In other words, rapamycin-induced Gat1-Myc^{13} binding upstream of *DAL5* was almost completely independent of Sit4, which was consistent with the predominantly nuclear and nuclear-cytoplasmic Gat1-Myc^{13} localization in rapamycin-treated wild type and *sit4*Δ cells (Fig. 3). Further, efficient Gat1-Myc^{13} binding did not require the presence of a second GATA factor, Gln3, because it occurred in the *gln3*Δ (Fig. 4*A* and supplemental Fig. S1). In contrast, Gln3-Myc^{13} binding to the *DAL5* promoter required not only Sit4, because of the necessity of the phosphatase for nuclear Gln3-Myc^{13} localization, but also the presence of Gat1, *i.e.* very little Gln3-Myc^{13} bound upstream of *DAL5* in a *gat1*Δ (Fig. 4*B* and supplemental Fig. S1).

To determine whether the loss of Gln3-Myc^{13} binding to *DAL5* in a *gat1*Δ derived from Gat1 being required for nuclear Gln3-Myc^{13} localization, we evaluated intracellular Gln3-Myc^{13} distribution. Deleting *GAT1* had little if any affect on nuclear Gln3-Myc^{13} localization following rapamycin treatment (Fig. 4, *C* and *D*).

DAL5 Transcription Remains Highly Rapamycin-inducible in Strains Lacking Ure2—The differences in Sit4 requirements for rapamycin-induced Gln3-Myc^{13} and Gat1-Myc^{13} localization and DNA binding prompted us to inquire whether Gln3 and Gat1 were also regulated differently downstream of Sit4, *i.e.* by Ure2.

Although recently questioned (15, 16, 22, 27, 29, 30–32, 45, 46), rapamycin was originally posited to abrogate excess nitrogen-dependent negative regulation of Sit4 by Tor1,2, thereby enabling Sit4 phosphatase to dephosphorylate Gln3 (8). This, in turn, brought about dissociation of the Gln3-Ure2 complex that permitted Gln3 to enter the nucleus. Importantly, Gat1 was reported to be similarly regulated (8). This model predicted that rapamycin-induced *DAL5* expression in a wild type strain would be the same as in an untreated or rapamycin-treated *ure2*Δ, where the Gln3-Ure2 and presumably Gat1-Ure2 interactions are lost. In other words, expression should be high and constitutive in the *ure2*Δ regardless of the conditions tested.

We tested this prediction using quantitative RT-PCR and Northern blot assays of *DAL5* transcription. As expected since

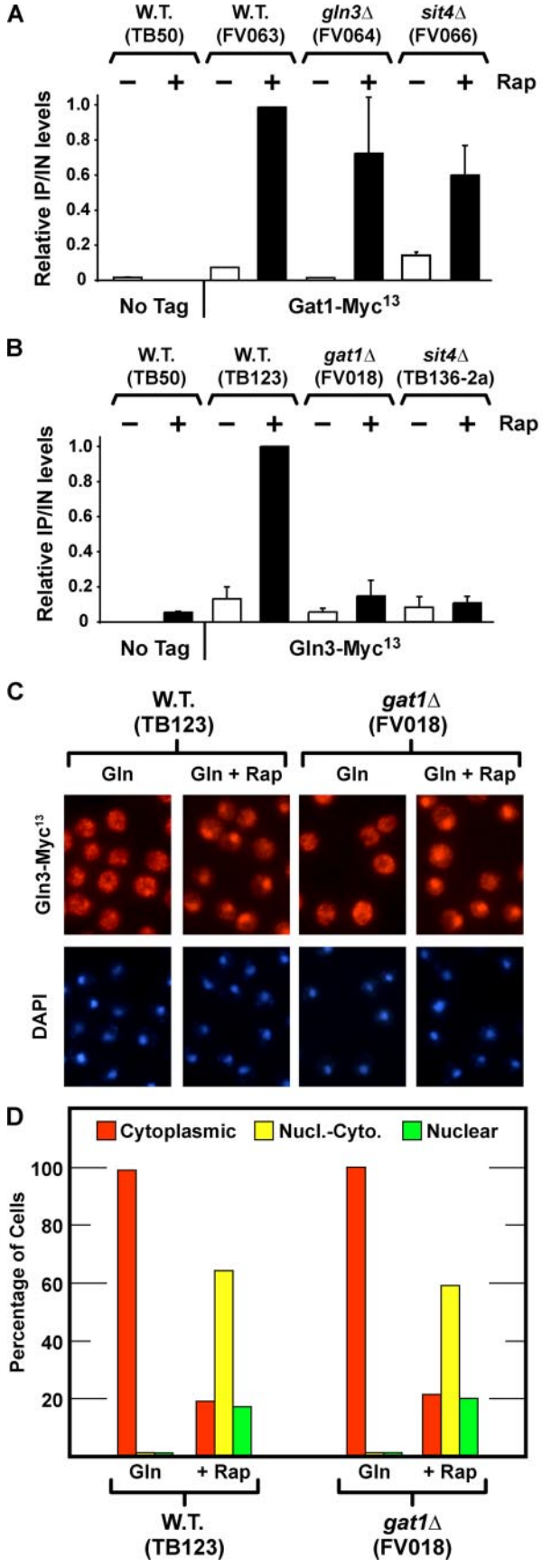

FIGURE 4. *A* and *B*, effects of *sit4*Δ, *gln3*Δ, and *gat1*Δ on rapamycin-induced binding of Gat1-Myc^{13} and Gln3-Myc^{13} to the *DAL5* promoter. *C* and *D*, effect of deleting *GAT1* on Gln3-Myc^{13} localization. Wild type (*W.T.*) untagged (TB50), wild type *GAT1-MYC*^{13} (FV063), *gln3*Δ *GAT1-MYC*^{13} (FV064), and *sit4*Δ *GAT1-MYC*^{13} (FV066) (*A*), and wild type untagged (TB50), wild type *GLN3-MYC*^{13} (TB123), *gat1*Δ *GLN3-MYC*^{13} (FV018), *sit4*Δ *GLN3-MYC*^{13} (TB136-2a) (*B*) strains were grown in YNB-glutamine medium with or without the addition of rapamycin (0.2 μg/ml) for 30 min. ChIP was performed using antibodies against c-Myc as described under "Materials and Methods." Quantitative PCR of IP and IN fractions was performed with primers for *DAL5* promoter (DAL5P) and for a region 2.5 kb upstream of *DAL5* open reading frame as a control (DAL5U). For each immunoprecipitation, IP/IN values were calculated as follows: $[DAL5P]^{IP}/[DAL5P]^{IN} - [DAL5U]^{IP}/[DAL5U]^{IN}$, normalized to the value obtained with wild type-induced cells. Histograms represent the average of at least two experiments from independent cultures. The *error bars* indicate standard errors. *C* and *D*, wild type and *gat1*Δ strains were grown in YNB-glutamine medium. Split cultures were left untreated (*Gln*) or treated with rapamycin (0.2 μg/ml) for 20 min (+*Rap*), sampled, and processed for immunofluorescence microscopy as described under "Materials and Methods" and in the legend to Fig. 3.

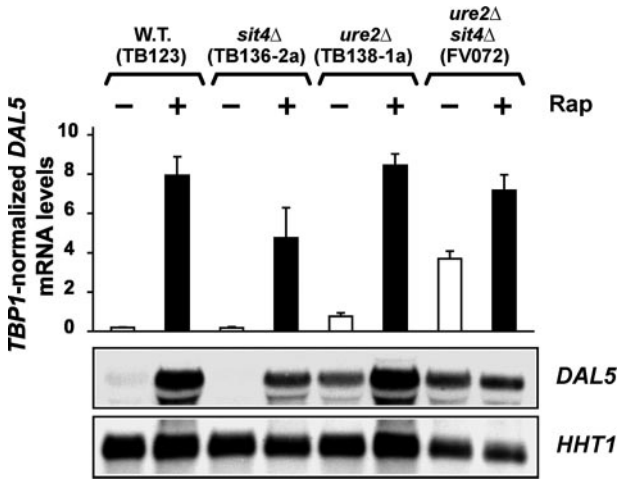

FIGURE 5. **Effects of *sit4*Δ, *ure2*Δ, and *sit4*Δ*ure2*Δ mutations on *DAL5* expression.** Total RNA was isolated from TB wild type (TB123), *sit4*Δ (TB136-2a) *ure2*Δ (TB138-1a), and *ure2*Δ*sit4*Δ (FV072) cells grown in YNB-glutamine medium that were untreated or treated with 0.2 μg/ml rapamycin for 30 min. The cells were treated, and analyses were performed as for Fig. 1. *W.T.*, wild type.

the initial discovery of the *ure2* locus (47, 48), deleting *URE2* increased *DAL5* expression in untreated, glutamine-grown cells (Fig. 5). Surprisingly, however, rapamycin treatment dramatically increased *DAL5* expression far beyond the level observed in an untreated *ure2*Δ and did so whether or not Sit4 was active (Fig. 5). *DAL5* transcription levels were nearly identical in rapamycin-treated wild type, *ure2*Δ, and *sit4*Δ*ure2*Δ cells. Beyond these remarkable observations, which we will address further below, we found that deleting both *SIT4* and *URE2* yielded a marked synergistic positive effect on *DAL5* transcription in untreated, glutamine-grown cells (Fig. 5). These results and their magnitude supported the idea that Tor1,2 regulation of *DAL5* transcription might be more complicated than simple Ure2-mediated control of intracellular GATA factor localization.

Gat1-Myc^{13} *and Gln3-Myc*^{13} *Localization Responds Differently to Deletion of Ure2*—To investigate the unexpected ability of rapamycin to greatly increase *DAL5* transcription in *ure2*Δ mutants, we focused on processes occurring between the action of Sit4 and *DAL5* transcription, *i.e.* intracellular GATA factor localization and binding to the *DAL5* promoter. To that end, we determined the effects of deleting *URE2* on Gln3-Myc^{13} and Gat1-Myc^{13} localization and then queried whether or not the

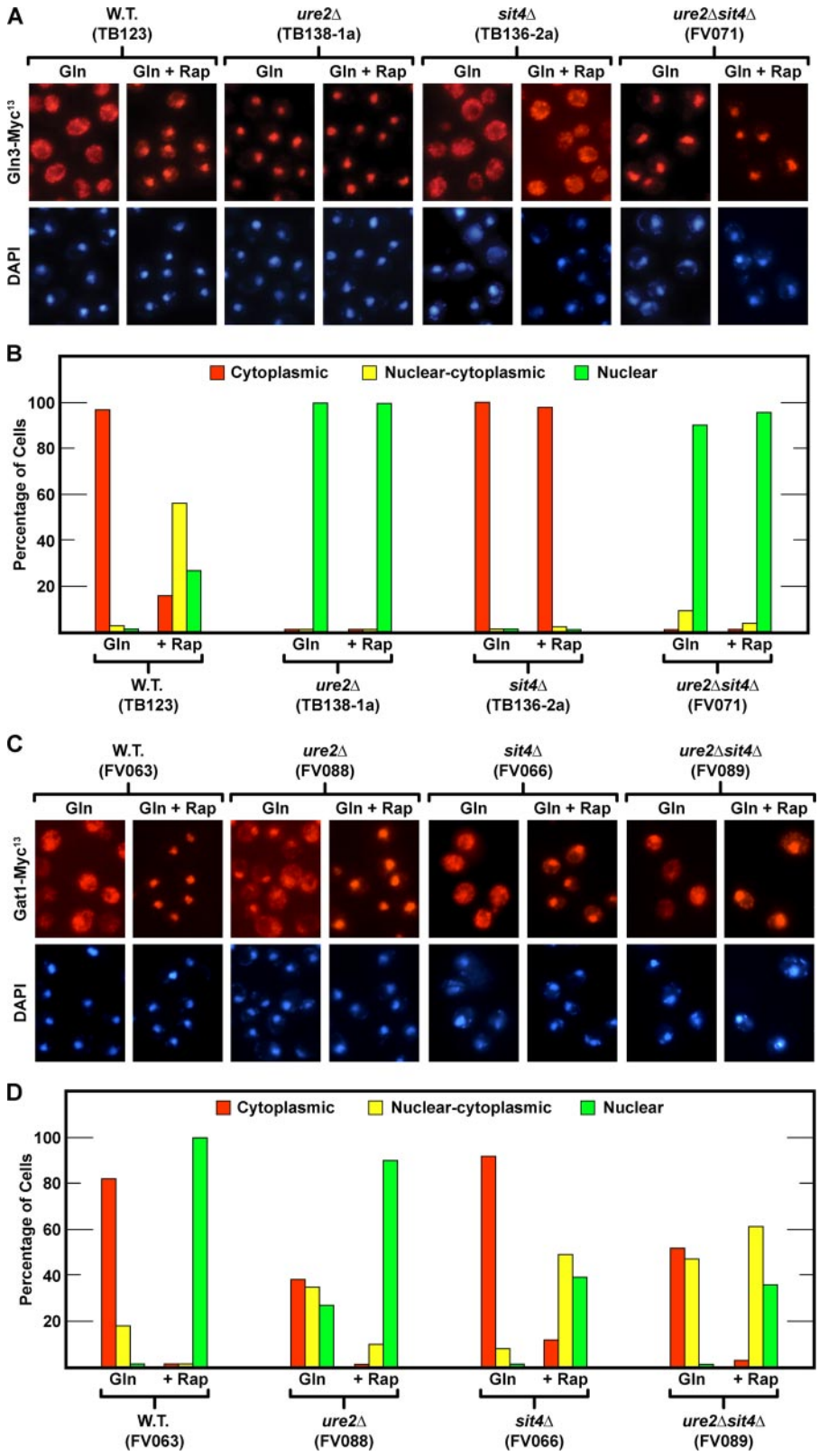

FIGURE 6. **Effects of rapamycin treatment on the intracellular localization of Gln3-Myc^{13} and Gat1-Myc^{13} in *ure2*Δ, *sit4*Δ, and *ure2*Δ*sit4*Δ mutant strains.** The formats for the experiments and presentation of the data were the same as in Fig. 3. *A* and *B*, Gln3-Myc^{13} was visualized. *C* and *D*, Gat1-Myc^{13} was visualized. Note that FV071 and FV072 have the same genotypes and were constructed in the same genetic background (see Table 1). In a similar experiment, FV072 gave results similar to those depicted here for FV071. *W.T.*, wild type.

absolute and limited Sit4 requirements observed for nuclear Gln3-Myc^{13} and Gat1-Myc^{13} localization, respectively, were abrogated in *ure2*Δ.

Gln3-Myc^{13} localization in glutamine-grown cells responded to deleting *URE2* as predicted, *i.e.* Gln3-Myc^{13} uniformly localized to the nuclei of essentially all *ure2*Δ cells whether or not they were treated with rapamycin, and in both cases Gln3-Myc^{13} was more nuclear than in rapamycin-treated wild type cells (Fig. 6, *A* and *B*, TB123 *versus* TB138-1a).

Parallel experiments demonstrated that Gat1-Myc^{13} localization was regulated quite differently. Although Gat1-Myc^{13} became a bit more nuclear in an untreated, glutamine-grown *ure2*Δ compared with wild type, *i.e.* the fraction of *ure2*Δ cells with nuclear-cytoplasmic or nuclear Gat1-Myc^{13} localization increased somewhat, it remained exclusively cytoplasmic in roughly 40% of the cells. This represented about a 2-fold decrease relative to wild type (Fig. 6, *C* and *D*, FV063 *versus* FV088). In other words, Gat1-Myc^{13} localization was not negatively regulated by Ure2 to the same degree as Gln3-Myc^{13}, where nuclear localization was observed in nearly all untreated *ure2*Δ cells (Fig. 6, compare *A* and *B* with *C* and *D*). Also in contrast with Gln3-Myc^{13}, the addition of rapamycin to the *ure2*Δ increased nuclear Gat1-Myc^{13} localization to the point where it was now nuclear in most cells just as in the wild type (Fig. 6, *C* and *D*, wild type +Rap *versus ure2*Δ +Rap). From these data we concluded that a protein other than or in addition to Ure2 was potentially responsible for maintaining Gat1-Myc^{13} in the cytoplasm of glutamine-grown cells and its ability to function depended upon Tor1,2, *i.e.* it too responded to rapamycin treatment.

Experiments addressing the epistasis of *ure2*Δ and *sit4*Δ mutations for Gln3-Myc^{13} localization showed that a *ure2*Δ was clearly epistatic to a *sit4*Δ in untreated and rapamycin-

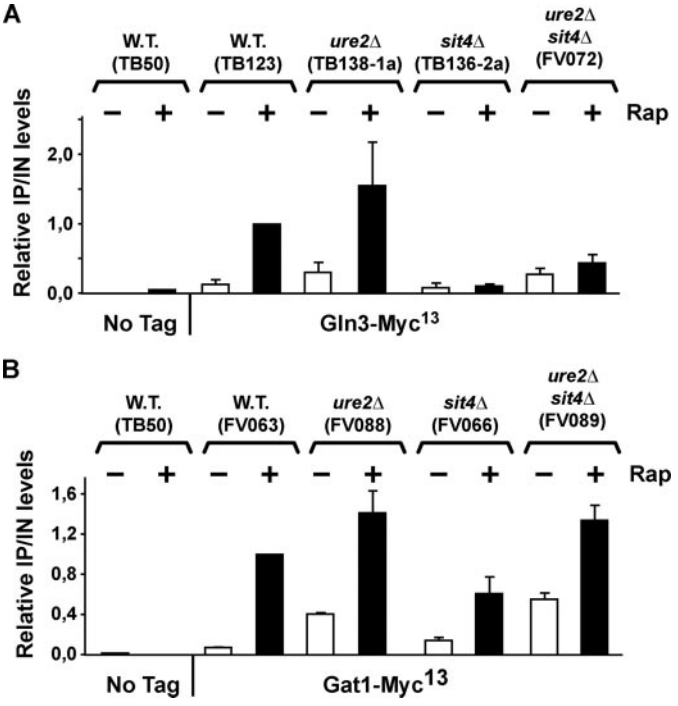

FIGURE 7. **ChIP analysis of rapamycin-induced recruitment of Gln3-Myc^{13} and Gat1-Myc^{13} to the *DAL5* promoters in wild type, *sit4*Δ, *ure2*Δ, and *ure2*Δ*sit4*Δ strains.** Wild type untagged (TB50), wild type *GLN3-MYC^{13}* (TB123), *ure2*Δ *GLN3-MYC^{13}* (TB138-1a), *sit4*Δ *GLN3-MYC^{13}* (TB136-2a), *ure2*Δ*sit4*Δ *GLN3-MYC^{13}* (FV072), wild type *GAT1-MYC^{13}* (FV063), *ure2*Δ *GAT1-MYC^{13}* (FV088), *sit4*Δ *GAT1-MYC^{13}* (FV066), and *ure2*Δ*sit4*Δ *GAT1-MYC^{13}* (FV089) strains were grown in YNB-glutamine medium with or without addition of rapamycin (0.2 μg/ml) for 30 min. ChIP and subsequent quantitative PCR were performed as in Fig. 4. *W.T.*, wild type.

treated glutamine-grown cells in that Gln3-Myc^{13} was cytoplasmic in the *sit4*Δ but nuclear in the *sit4*Δ*ure2*Δ double mutant. The parallel epistasis analysis of Gat1-Myc^{13} localization yielded results that were much less straightforward than with Gln3-Myc^{13}, again pointing to differences in their regulation. The untreated *sit4*Δ*ure2*Δ mutant phenotype was overall perhaps more like that of the *ure2*Δ than the *sit4*Δ, whereas the rapamycin-treated *sit4*Δ*ure2*Δ behaved more like a *sit4*Δ. In neither case were the phenotypes sufficiently strong or different to confidently draw firm conclusions about epistasis. What could be confidently concluded was that Sit4 and Ure2 exerted much less control over Gat1-Myc^{13} than Gln3-Myc^{13} localization.

More Than Gln3-Myc^{13} Nuclear Localization Is Required for It to Bind to the DAL5 Promoter—We finally investigated Sit4- and Ure2-mediated regulation of Gln3-Myc^{13} and Gat1-Myc^{13} interactions with the *DAL5* promoter (Fig. 7 and supplemental Fig. S2). Using ChIP assays, we performed epistasis experiments parallel to those described in Fig. 6. The most striking and unexpected observation was that nuclear Gln3-Myc^{13} localization and binding to the *DAL5* promoter did not correlate with one another. Gln3-Myc^{13} was uniformly nuclear in both untreated and rapamycin-treated *ure2*Δ cells (Fig. 6, *A* and *B*). In contrast, its binding to the *DAL5* promoter remained rapamycin-inducible (Fig. 7*A*).

In another example, Gln3-Myc^{13} binding to the *DAL5* promoter was 3-fold less in an untreated *ure2*Δ compared with the rapamycin-treated wild type (Fig. 7*A* and supplemental Fig. S2), whereas nuclear Gln3-Myc^{13} localization was greater in the former instance than in the latter (Fig. 6, *A* and *B*). In yet a third example, the addition of a *sit4*Δ to a *ure2*Δ strain substantially diminished Gln3-Myc^{13} binding to the *DAL5* promoter in rapamycin-treated cells (Fig. 7*A* and supplemental Fig. S2), despite its exclusively nuclear localization (Fig. 6, *A* and *B*). These failed correlations indicated that more than just nuclear Gln3-Myc^{13} localization dictated its binding to *DAL5* DNA especially in the presence of rapamycin. Moreover, this binding was somehow influenced by Sit4.

There was, however, one positive correlation we could see in the *ure2*Δ strains. Increased Gln3-Myc^{13} binding to the *DAL5* promoter following the addition of rapamycin to a *ure2*Δ correlated with rapamycin-induced nuclear Gat1-Myc^{13} localization under the same conditions, which is in agreement with the observation that Gln3-Myc^{13} binding to the *DAL5* promoter requires Gat1.

In contrast with Gln3-Myc^{13}, more positive correlations were observed with Gat1-Myc^{13}. Gat1-Myc^{13} binding to the *DAL5* promoter in untreated and rapamycin-induced *ure2*Δ cells (Fig. 7*B* and supplemental Fig. S2) roughly paralleled its nuclear localization and Gat1-supported transcription (Figs. 5 and 6, *C* and *D*). Nevertheless, rapamycin-induced Gat1-Myc^{13} binding to the *DAL5* promoter in a *ure2*Δ*sit4*Δ was comparable with that in a *ure2*Δ, even though somewhat less Gat1-Myc^{13} was present in the nucleus in the former situation.

DISCUSSION

The most important mechanistic outcome of the above experiments is their demonstration that the Tor1,2 signal transduction pathway bifurcates at the level of GATA factor regulation in *S. cerevisiae* (Fig. 8). This conclusion is supported by three main lines of evidence: (i) rapamycin-induced nuclear Gln3-Myc^{13} localization in glutamine-grown cells possesses an absolute requirement for the type 2A-related phosphatase, Sit4, whereas nuclear Gat1-Myc^{13} localization exhibits only a limited Sit4 requirement at best; (ii) intracellular Gat1-Myc^{13} localization is largely immune to regulation by Ure2, the highly effective negative regulator absolutely required to sequester Gln3-Myc^{13} in the cytoplasm of cells provided with a good nitrogen source; and (iii) Gln3-Myc^{13} binding to the *DAL5* promoter requires the presence of Gat1, but Gat1-Myc^{13} binds to this DNA independently of Gln3.

Previous reports forecast that differences in Gln3 and Gat1 regulation might exist and encouraged us to look for them. Although a Ure2-Gln3-Myc^{13} complex was straightforwardly identified by *in vitro* co-immunoprecipitation (8, 11, 19), repeated attempts to identify a similar Ure2-Gat1 complex were unsuccessful (8, 11). Additionally, *in vivo* rapamycin-induced and *in vitro* alkaline phosphatase-dependent dephosphorylation of Gln3-Myc^{13} was easily demonstrated (8, 11, 33, 46). In contrast, similar attempts to demonstrate Gat1-Myc^{13} phosphorylation and rapamycin-induced dephosphorylation were unsuccessful, even though Gat1-Myc^{13} phosphorylation *per se*, *i.e.* Snf1-dependent Gat1-Myc^{13} phosphorylation, could be readily detected (33).

The above evidence demonstrating regulatory bifurcation of GATA factor regulation additionally raises significant new pos-

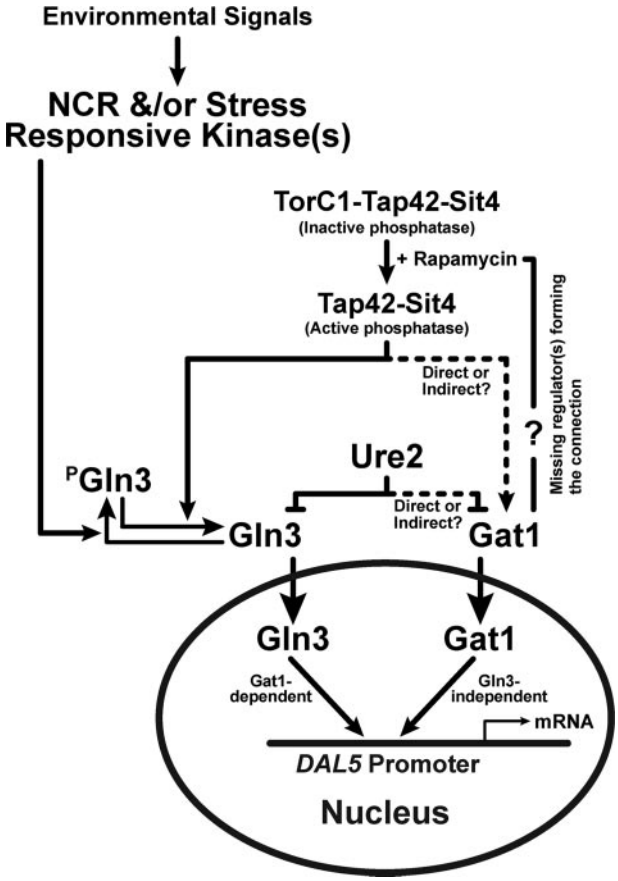

FIGURE 8. **Diagrammatic summary of data, showing bifurcation of Tor pathway at the level of GATA factor regulation.** The *arrows* and *bars* indicate positive and negative regulation, respectively. The absence of *arrows* or *bars* indicates insufficient data are available to make such a characterization. This diagrammatic summary does not address the molecular mechanism of Gln3 regulation by Ure2 (two models have been suggested (8, 11)) or the transfer of environmental signals to Tor1,2 and other protein kinases.

sibilities and questions. If the overall mechanisms of Gln3 and Gat1 regulation in response to rapamycin treatment are analogous, at least two components participating in Tor1,2 regulation of GATA factor localization likely remain to be identified: (i) molecule(s) responsible for Gat1-Myc^{13} sequestration in the cytoplasm of cells provided with good nitrogen sources, the functional counterpart of Ure2, and (ii) molecule(s) forming the regulatory connection between the site of rapamycin action, presumably the TorC1-Tap42-phosphatase complex, and the molecule(s) responsible for sequestering Gat1 in the cytoplasm during growth with excess nitrogen. The working diagram in Fig. 8 portrays this connection, but the lack of pertinent data does not justify defining it further.

A related question is prompted by the modest effects of *sit4*Δ and *ure2*Δ mutations on Gat1-Myc^{13} regulation. Do the phenotypes generated by these mutations derive from direct control of Gat1-Myc^{13} by Sit4 and Ure2 or alternatively represent indirect secondary effects? Stated in another way, do Sit4, Ure2, plus unknown proteins with analogous and somewhat redundant functions jointly regulate Gat1-Myc^{13}? Alternatively, do these unknown regulatory proteins alone regulate Gat1-Myc^{13} and observed influences of the *sit4*Δ and *ure2*Δ derive as indirect consequences of regulatory cross-talk between branches of the bifurcated pathway?

Two earlier observations will likely have an impact on the answers to these questions: (i) Gat1-mediated expression of multiple genes associated with the transport and metabolism of nitrogenous compounds remains highly NCR-sensitive in a *gln3*Δ*ure2*Δ mutant (41–44) and (ii) overexpression of Ure2 can restrict EGFP-Gat1 to the cytoplasm under conditions in which it would otherwise be nuclear (49).

Next, two sets of correlations prompt us to speculate that Gat1-Myc^{13} and Gln3-Myc^{13} may positively influence one another's binding to the *DAL5* promoter, conceivably through protein-protein interactions: (i) Following entry of the GATA factors into the nucleus, rapamycin induces Gat1-Myc^{13} binding to the *DAL5* promoter independently of Gln3, whereas Gln3-Myc^{13} binding requires Gat1. In other words, gaining entry to the nucleus in response to rapamycin treatment is alone insufficient to bring about Gln3-Myc^{13} binding to the *DAL5* promoter. Further, even though Gln3-Myc^{13} is fully nuclear in a *ure2*Δ, its binding to the *DAL5* promoter was much less than observed when rapamycin was present, *i.e.* when Tor1,2 regulation was abrogated. This increased rapamycin-induced Gln3-Myc^{13} binding correlates with parallel increases in nuclear Gat1-Myc^{13} localization and binding to the *DAL5* promoter in response to rapamycin addition. (ii) Conversely, increased nuclear Gln3-Myc^{13} localization that occurs in the *sit4*Δ*ure2*Δ relative to a *sit4*Δ and the roughly 2-fold greater Gln3-Myc^{13} binding to *DAL5* in a *ure2*Δ*sit4*Δ relative to that in a *sit4*Δ correlates with the roughly 2-fold increased Gat1-Myc^{13} binding to the *DAL5* promoter in the double mutant.

If the possibility that Gat1 and Gln3 do interact with one another and thereby reciprocally promote each other's binding to the promoter is valid, it would contribute significantly toward explaining these correlations. That said, data supporting a positive effect of Gat1-Myc^{13} on Gln3-Myc^{13} binding to the *DAL5* promoter are certainly stronger than those arguing in favor of the converse situation.

As we speculate about such models of GATA factor control, however, we keep two important caveats firmly in mind: (i) because of the unexpectedly high occurrence of strain-specific variations in nitrogen-responsive regulation, general characteristics of NCR-sensitive, GATA factor control must be distinguished from strain-specific traits (45), and (ii) models describing intra-nuclear GATA factor regulation must take the structures of the particular promoters being studied into account. For example, *DAL5* is among the simplest of the NCR-sensitive promoters, and for that reason it is often used as a NCR-sensitive reporter. A small fragment of the *DAL5* promoter, containing two functional GATAA sequences, is necessary and sufficient to support NCR-sensitive transcription in a heterologous expression vector assay (50). With more complex promoters, Gln3 binding to DNA may require one or more non-GATA factor DNA-binding proteins. Examples of this phenomenon have been observed with *DAL7*, *PUT1*, and *GLN1* promoter fragments (26, 51).

Finally, multiple observations made in this work lead us to suspect that there may be yet undiscovered rapamycin-induced and/or Sit4-controlled events that regulate rapamycin-induced *DAL5* transcription beyond the point of GATA factor entry into the nucleus. The most indicative observations of this pos-

sibility are the multiple effects of rapamycin addition and *SIT4* deletion in *ure2*Δ strains. Such putative events could potentially occur at the level of GATA factor binding to the regulated gene promoter or thereafter at the level of transcriptional activation. Our observations also demonstrate that gross transcription levels of nitrogen-responsive genes are alone unlikely to be unambiguous reporters of Tor1,2 pathway regulation.

Acknowledgments—We thank Dr. Michael Hall for strains, Tim Higgins and André Feller for preparing the artwork, Fabienne Vierendeels for excellent technical assistance, Maxime Wéry for helpful advice on ChIP experiments, and the University of Tennessee Yeast Group for suggestions to improve the manuscript.

REFERENCES

1. Schluter, M., and Schofer, J. (2005) *Am. Heart Hosp. J.* **3,** 182–186
2. Boulay, A., Rudloff, J., Ye, J., Zumstein-Mecker, S., O'Reilly, T., Evans, D. B., Chen, S., and Lane, H. A. (2005) *Clin. Cancer Res.* **11,** 5319–5328
3. Morgensztern, D., and McLeod, H. L. (2005) *Anticancer Drugs.* **16,** 797–803
4. Lorber, M. I., Mulgaonkar, S., Butt, M., Elkhammas, E., Mendez, R., Rajagopalan, P. R., Kahan, B., Sollinger, H., Li, Y., Cretin, N., and Tedesco, H. (2005) *Transplantation* **80,** 244–252
5. Thomas, G., Sabatini, D., and Hall, M. N. (eds) (2004) *Current Topics in Microbiology and Immunology: Target of Rapamycin,* Springer, New York
6. Inoki, K., Ouyang, H., Li, Y., and Guan, K. L. (2005) *Microbiol. Mol. Biol. Rev.* **69,** 79–100
7. Cooper, T. G. (2004) in *Nutrient-Induced Responses in Eukaryotic Cells Current Genetics* (Winderickx, J., and Taylor, P. M., eds) Vol. 7, Chapter 9, pp. 225–257, Springer-Verlag Berlin
8. Beck, T., and Hall, M. N. (1999) *Nature* **402,** 689–692
9. Cardenas, M. E., Cutler, N. S., Lorenz, M. C., Di Como, C. J., and Heitman, J. (1999) *Genes Dev.* **13,** 3271–3279
10. Hardwick, J. S., Kuruvilla, F. G., Tong, J. K., Shamji, A. F., and Schreiber, S. L. (1999) *Proc. Natl. Acad. Sci. U. S. A.* **96,** 14866–14870
11. Bertram, P. G., Choi, J. H., Carvalho, J., Ai, W., Zeng, C., Chan, T. F., and Zheng, X. F. (2000) *J. Biol. Chem.* **275,** 35727–35733
12. Cox, K. H., Rai, R., Distler, M., Daugherty, J. R., Coffman, J. A., and Cooper, T. G. (2000) *J. Biol. Chem.* **275,** 17611–17618
13. Kuruvilla, F. G., Shamji, A. F., and Schreiber, S. L. (2001) *Proc. Natl. Acad. Sci. U. S. A.* **98,** 7283–7288
14. Rohde, J. R., Campbell, S., Zurita-Martinez, S. A., Cutler, N. S., Ashe, M., and Cardenas, M. E. (2004) *Mol. Cell Biol.* **24,** 8332–8341
15. Tate, J. J., and Cooper, T. G. (2003) *J. Biol. Chem.* **278,** 36924–36933
16. Giannattasio, S., Liu, Z., Thornton, J., and Butow, R. A. (2005) *J. Biol. Chem.* **280,** 42528–42535
17. Hofman-Bang, J. (1999) *Mol. Biotechnol.* **12,** 35–73
18. Magasanik, B., and Kaiser, C. A. (2002) *Gene* (*Amst.*) **290,** 1–18
19. Blinder, D., Coschigano, P. W., and Magasanik, B. (1996) *J. Bacteriol.* **178,** 4734–4736
20. Kulkarni, A. A., Abul-Hamd, A. T., Rai, R., El Berry, H., and Cooper, T. G. (2001) *J. Biol. Chem.* **276,** 32136–32144
21. Di Como, C. J., and Arndt, K. T. (1996) *Genes Dev.* **10,** 1904–1916
22. Jiang, Y., and Broach, J. R. (1999) *EMBO J.* **18,** 2782–2792
23. Jacinto, E., Guo, B., Arndt, K. T., Schmelzle, T., and Hall, M. N. (2001) *Mol. Cell* **8,** 1017–1026
24. Carvalho, J., and Zheng, X. F. (2003) *J. Biol. Chem.* **278,** 16878–16886
25. Crespo, J. L., Helliwell, S. B., Wiederkehr, C., Demougin, P., Fowler, B., Primig, M., and Hall, M. N. (2004) *J. Biol. Chem.* **279,** 37512–37517
26. Rai, R., Daugherty, J. R., and Cooper, T. G. (1995) *Yeast* **11,** 247–260
27. Wang, H., Wang, X., and Jiang, Y. (2003) *Mol. Biol. Cell* **14,** 4342–4351
28. Crespo, J. L., Powers, T., Fowler, B., and Hall, M. N. (2002) *Proc. Natl. Acad. Sci. U. S. A.* **99,** 6784–6789
29. Tate, J. J., Rai, R., and Cooper, T. G. (2005) *J. Biol. Chem.* **280,** 27195–27204
30. Tate, J. J., Feller, A., Dubois, E., and Cooper, T. G. (2006) *J. Biol. Chem.* **281,** 37980–37992
31. Feller, A., Boeckstaens, M., Marini, A. M., and Dubois, E. (2006) *J. Biol. Chem.* **281,** 28546–28554
32. Tate, J. J., Rai, R., and Cooper, T. G. (2006) *J. Biol. Chem.* **281,** 28460–28469
33. Kulkarni, A., Buford, T. D., Rai, R., and Cooper, T. G. (2006) *FEMS Yeast Res.* **6,** 218–229
34. Scherens, B., Feller, A., Vierendeels, F., Messenguy, F., and Dubois, E. (2006) *FEMS Yeast Res.* **6,** 777–791
35. Wach, A. (1996) *Yeast* **12,** 259–265
36. Longtine, M. S., McKenzie, A. 3rd, Demarini, D. J., Shah, N. G., Wach, A., Brachat, A., Philippsen, P., and Pringle, J. R. (1998) *Yeast* **14,** 953–961
37. Schmitt, M. E., Brown, T. A., and Trumpower, B. L. (1990) *Nucleic Acids Res.* **18,** 3091–3092
38. Foury, F., and Talibi, D. (2001) *J. Biol. Chem.* **276,** 7762–7768
39. Cox, K. H., Tate, J. J., and Cooper, T. G. (2002) *J. Biol. Chem.* **277,** 37559–37566
40. Tate, J. J., and Cooper, T. G. (2007) *J. Biol. Chem.* **282,** 18467–18480
41. Coffman, J. A., Rai, R., Cunningham, T., Svetlov, V., and Cooper, T. G. (1996) *Mol. Cell Biol.* **16,** 847–858
42. Coffman, J. A., el Berry, H. M., and Cooper, T. G. (1994) *J. Bacteriol.* **176,** 7476–7483
43. Coffman, J. A., Rai, R., and Cooper, T. G. (1995) *J. Bacteriol.* **177,** 6910–6918; Correction (1996) *J. Bacteriol.* **178,** 2159
44. Coffman, J. A., Rai, R., Loprete, D. M., Cunningham, T., Svetlov, V., and Cooper, T. G. (1997) *J. Bacteriol.* **179,** 3416–3429
45. Tate, J. J., Cox, K. H., Rai, R., and Cooper, T. G. (2002) *J. Biol. Chem.* **277,** 20477–20482
46. Cox, K. H., Kulkarni, A., Tate, J. J., and Cooper, T. G. (2004) *J. Biol. Chem.* **279,** 10270–10278
47. Drillien, R., and Lacroute, F. (1972) *J. Bacteriol.* **109,** 203–208
48. Drillien, R., Aigle, M., and Lacroute, F. (1973) *Biochem. Biophys. Res. Commun.* **53,** 367–372
49. Cunningham, T. S., Andhare, R., and Cooper, T. G. (2000) *J. Biol. Chem.* **275,** 14408–14414
50. Cooper, T. G., Rai, R., and Yoo, H. S. (1989) *Mol. Cell Biol.* **9,** 5440–5444
51. Rai, R., Daugherty, J. R., Cunningham, T. S., and Cooper, T. G. (1999) *J. Biol. Chem.* **274,** 28026–28034